Dip-coating of yield stress fluids

Mathilde Maillard, Jeremy Bleyer, A.L. Andrieux, Jalila Boujlel, Philippe Coussot

Dip-coating of yield stress fluids

M. Maillard, J. Bleyer, A.L. Andrieux, J. Boujlel*, P. Coussot

Université Paris-Est, Laboratoire Navier, Champs sur Marne, France

* IFPEN, Rueil-Malmaison, France

Abstract: We review and discuss the characteristics of dip-coating of yield stress fluids on the basis of theoretical considerations, numerical simulations of the flow in the bath and experimental data with different materials. We show that in general, due to the yield stress, viscous dissipations are sufficiently large for capillary effects to be negligible in the process. Dip-coating with yield stress fluids is thus essentially governed by an equilibrium between viscous and gravity effects. In contrast with simple liquids the coated thickness is uniform and remains fixed to the plate. At low velocities it appears to tend to a value significantly smaller than the Derjaguin and Levi prediction [B.V. Derjaguin, S.M. Levi, *Film coating theory* (The Focal Press, London, 1964)], i.e. critical thickness of stoppage of a free surface flow along a vertical plate. We show that this comes from the fact that in the bath only a relatively small layer of fluid is in its liquid regime along the moving plate while the rest of the material is in a solid regime. From numerical simulations we describe the general trends of this liquid layer and in particular its thickness as a function of the rheological characteristics and plate velocity. We finally propose a model for the dip-coating of yield stress fluid, assuming that the solid volume of fluid finally fixed to the plate results from the mass flux of the liquid layer in the bath minus a mass flux due to some downward flow under gravity in the transition zone. A good agreement between this model and experimental data is found for a yield stress larger than 20 Pa.

1. Introduction

Yield stress fluids (YSF) are encountered in a wide range of applications: toothpastes, cements, mortars, foams, muds, mayonnaise, etc. The fundamental character of these fluids is that they are able to flow (i.e., deform indefinitely) only if they are submitted to a stress above some critical value, i.e. their yield stress. Otherwise they deform in a finite way like solids. The flow characteristics of such materials are difficult to predict as they involve permanent or transient solid and liquid regions that are generally hard to locate a priori [1].

In our everyday life we commonly extract objects from baths of yield stress fluids (mud, chocolate, paint, cement paste, cream, etc). A significant layer of fluid remains on the tool, which is then coated over some other solid surface (bread, wall, skin, etc). The first part of this operation is the well-known dip-coating process. Various industrial processes (food industry, automobile) rely on this technique for coating or treating the surfaces. The stake of research in that field is to understand the fluid flow under the effect of the solid displacement to optimize the process parameters: geometrical dimensions of the solid coated and container, distance between the solids, velocity of the object to coat, rheological characteristics of the fluid.

In the case of simple liquids the flow resulting the object extraction is described as the Landau-Levich problem. Dip coating of plates or cylinders with Newtonian liquids (of viscosity μ) has been the object of much research and there now exists a solid background of knowledge. Most studies in that field focused on the film formation and thickness [2-4]. The value of the film

thickness results from a balance between gravity, capillary and viscous effects. Different flow regimes may be observed inside the bath, but it is worth emphasizing that the liquid flows at any point [5], so that the transition from the bath to the surface is smooth.

A limited number of (phenomenological) studies concerned non-linear fluids. No unified conclusion was reached for the dip-coating of plates: for a shear-thinning behavior a thickness increase [6-7] or decrease [8-10] was observed, numerically or experimentally, when the power-law index decreases. For fibers, it was shown that elastic effects tend to increase the value of the coated thickness h [11-12].

For yield stress fluids previous works on dip-coating are scarce. A theoretical approach suggested that the coated layer thickness is larger as a result of the yield stress [10] and some numerical simulations [13-14] suggested that h increases with τ_c and that surface tension effects are negligible. Another theoretical analysis [15] in the case of dominant yielding effect (i.e. plastic flow) and negligible gravity effects finally predicted that $h \propto \tau_c^2$. Finally the first experimental study with yield stress fluids showed that the coated layer remains stuck on the plate after its withdrawal, and that the coated thickness is approximately proportional to the yield stress of the material [16]. Moreover, from a global analysis of the velocity field for one yield stress fluid it was suggested that the coated thickness is related to the flow characteristics inside the bath.

The purpose of the present paper is to review the problem of dip-coating with yield stress fluids in a more general way. In that aim we will rely on theoretical considerations, previous and new experimental data, and numerical simulations of the flow in the bath. We will start by positioning the problem by taking advantage of existing knowledge for simple fluids and emphasizing the differences with yield stress fluids. We will then discuss the different possible flow regimes as a function of the relative importance of capillary, gravity and viscous effects. At last we will discuss in more details the origin of the value of the coated thickness, in relation with the flow characteristics inside the bath (in particular the thickness of the sheared layer along the plate).

2. Theoretical considerations

2.1 The material

In order to understand the rheological behavior of a yield stress fluid, a good way consists in applying different stress levels to it, starting always from the same initial state (for example after some fluid mixing), and looking at the deformation in time. After a transient stage, the different deformation vs time curves evolve in two ways (see [17]). For a stress above a critical value they end up with unit slope on a logarithmic scale, indicating that the material flows at a constant shear rate. We thus consider the material to be in its *liquid regime*. For a lower stress, the deformation seems to tend to a plateau, and remains below a critical value, as it would for

a solid. More precisely the deformation goes on increasing in time, suggesting a very slow flow, but the apparent shear rate continues to decrease in time towards lower and lower values, without reaching a steady state flow. The apparently limited deformation and continuous decrease in the apparent shear rate towards very low values justifies treating this as a *solid regime*. The maximum deformation that can be reached in the solid regime, i.e. for a stress just below the yield stress, is the critical deformation.

The surprising feature of yield stress fluids is that: (i) they exhibit a solid structure at rest, which may be understood using the same framework as standard solids; (ii) beyond the critical deformation, this structure breaks down and the material flows like a simple fluid; (iii) if the material is left at rest once again, it recovers its initial mechanical (solid) properties, associated with a similar structure. We thus have a material able to move from a solid to a liquid state, and from a liquid to a solid state, in a reversible way. Such a situation probably results from soft interactions between the elements composing the fluid. These elements may form a jammed (solid) structure, which can easily break if subjected to high enough stress. The breakage assumed here is a kind of homogeneous plastic flow (with plastic events well dispersed throughout the material). It is not yet clear whether such a situation effectively takes place at very low shear rates.

Such a description seems to apply well to materials such as foams, gels, and emulsions, but not as simply to colloidal suspensions, whose structure may significantly evolve at rest as a result of colloidal interactions and Brownian agitation. In that case the transition between the solid and the liquid regimes as described above seems to be more "abrupt". In a series of creep tests, a jump appears between the two regions, and this means that no steady state can be reached at a shear rate below the critical value [18]. Such behavior is thought to be intimately associated with the *thixotropic* character of the fluid [19], i.e., the time-dependence of the material properties. An important consequence is that one cannot so easily define the yield stress of the material. Starting from rest, we may identify a *static yield stress*, i.e., the critical stress allowing steady state flow, but this can vary significantly depending on how long the material was previously left at rest (since the structure will have strengthened in time), and it differs from the *dynamic yield stress* associated to flow stoppage.

Here we will focus mainly on the flow characteristics of non-thixotropic yield stress fluids which to a good first approximation can be described as *simple yield stress fluids* [20-21], and for which the dynamic yield stress is close to the static yield stress. A broad range of data gathered over the past twenty years has shown that, for shear rates in the range $\left[0.01;100\mathrm{s}^{-1}\right]$, the rheological behavior of simple yield stress fluids in steady state simple shear can be very well represented by the Herschel-Bulkley (HB) model, which can be stated as follows:

$$\tau < \tau_c \Rightarrow \dot{\gamma} = 0 \text{ (solid regime)}; \quad \tau > \tau_c \Rightarrow \tau = \tau_c + k\dot{\gamma}^n \text{ (liquid regime)} \qquad (1)$$

Here τ is the shear stress amplitude, $\dot{\gamma}$ the shear rate amplitude, τ_c the yield stress, and k and n two material parameters. A 3D tensorial expression can be extrapolated from (1) with the help of a von Mises criterion for the solid-liquid transition [22]. The parameter n generally lies in the range [0.3; 0.5]. Most work has focused on behavior in the liquid regime. Note that yield stresses below 1 Pa are hardly detectable by usual rheometrical tests due to artefacts. As a consequence in order to be sure to deal with true yield stress fluids with properly determined rheological parameters it is preferable to use materials exhibiting a yield stress larger than a few Pascals. Few works focused on the rheological properties of yield stress fluids in the solid regime but they suggest that these properties are similar to those of usual solids, ranging from almost pure linear elasticity to complex viscoelastoplasticity.

In the context of laminar flows of yield stress fluids, a dimensionless number turns out to be of fundamental interest for characterizing the physics of the flow. This is the Bingham number, $Bi = \tau_c / k\dot{\gamma}^n$, which estimates the ratio of the constant part of the constitutive equation in the liquid regime - which may be related to the strength of the solid structure as it also corresponds to the critical stress for the solid-liquid transition - to the rate-dependent (viscous) part of this constitutive equation. Since the stress distribution in flows are in general heterogeneous a liquid and a solid regions coexist. As a consequence, if we take for $\dot{\gamma}$ the ratio of a characteristic velocity to a characteristic distance between flow boundaries, the Bingham number gives some measure of the relative importance of the solid and liquid regions in the sample. Indeed, for example in a channel flow when $Bi \to \infty$ most of the fluid is in its solid regime whereas when $\mathrm{Bi} \to 0$ most of the fluid is in its liquid regime.

2.2 The boundary conditions

The situation we study here is a plate immersed in a bath of fluid (in a container) perpendicularly to its free surface (see Figure 1). The width of the plate is assumed to be sufficiently large for the flow to be essentially 2D, so that all descriptions in this paper will assume that all flow characteristics are similar along a *z*-axis (perpendicular to a plane of visualization as in Figure 1). At the initial time the plate is withdrawn vertically from the bath. For simple liquids the history of plate displacement through the bath has no impact on the process, since such a fluid immediately forgets it flow history. For a YSF the situation is different: after immersion the plate must be left at rest some time to let the material reach its solid regime and, if possible, relax residual stresses. The data on that point nevertheless show that beyond a short time at rest there is no impact of the resting time on the flow characteristics inside and outside the bath [23-24]. Note that on the contrary for thixotropic YSF this point would likely be critical: the static yield stress increases with the time of rest after mixing, which will strongly affect the coating process.

Another more complex aspect with YSF concerns the container geometry. For simple liquids, if the coated layer thickness is much smaller than the distance between the plate and the walls of the container the impact of the container size is negligible. For yield stress fluids the stress distribution which depends on boundary conditions determines the distribution of liquid and solid regions and thus may have a significant impact on the flow along the plate.

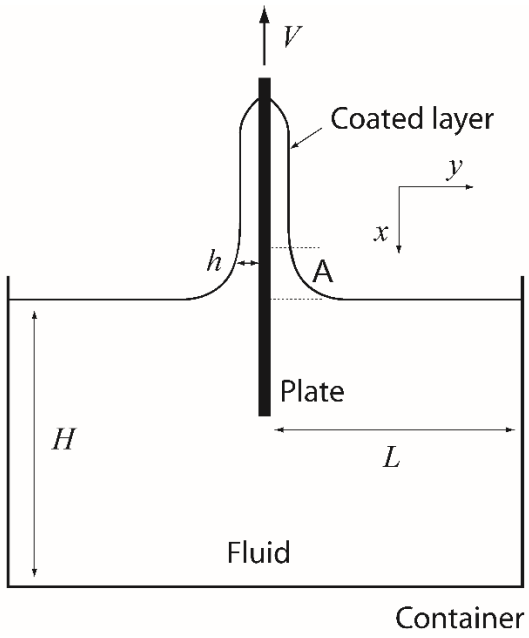

Figure 1: Scheme of the dip-coating experiment.

Yield stress fluids are necessarily composed of elements of size much larger than the atomic size and interacting in such a way that they can make a jammed structure. Such elements are for example colloidal particles, bubbles, droplets, grains, etc, which may have a size up to several tenths of microns. As a consequence, for the continuum assumption to remain valid during the coating process the thickness of the coated film must be much larger than the element size. Fortunately, likely as a result of the yield stress, we will see that the coated thickness of YSF is typically of millimetric size, which generally ensures the validity of this assumption.

These characteristics of YSF are also at the origin of an effect which may have a critical impact on the dip-coating process: wall slip. Since the elements are in general suspended in a liquid their concentration can decrease at the approach of the wall thus forming a less viscous fluid layer which will be preferentially sheared. In an extreme case only this thin layer is sheared while the rest of the material moves as a plug. Such a phenomenon can generally be avoided by using rough wall surfaces, which allows the elements to be homogeneously dispersed throughout the virtual boundary surface (envelop of the rough surface) [22]. Ideal wall slip during dip-coating will just lead to coat a very thin layer of the interstitial liquid of the YSF.

Here we will assume that no wall slip occurs, i.e. rough surfaces with a roughness much larger than the element size are used. In this situation it will be relevant to consider the flow in the frame of continuum mechanics and see the plate surface as a perfect plane only if the coated thickness is much larger than this roughness.

2.3 Main forces acting in the process

As for any type of fluid, in this problem mainly three effects can play a role: capillary, gravity and viscous effects. Let us first consider capillary effects. Although YSF are fundamentally composite systems made of elements in strong interactions at the origin of the yield stress existing measures tend to suggest that the surface tension (σ) of model YSF is close to that of the interstitial liquid [25-26]. Measurements nevertheless remain difficult since, even for very slow flows viscous effects can be large as the stress is necessarily above the yield stress in the flowing regions. In order to measure surface tension it is thus necessary to minimize the viscous dissipation by decreasing the fluid volume relatively to the area of its interface [25].

In order to compare capillary to viscous effects during dip-coating we consider the fluid volume in the transition zone (A) situated between the initially horizontal free surface of the bath and the uniform coated thickness region (see Figure 1). We assume that the height of this region is of the order of the thickness of the fluid layer on the plate, h. An elementary vertical displacement of the plate of dx induces basically a shear of the material with a deformation approximately equal to dx/h, which is associated to a viscous dissipation of the order of $\tau_c(dx/h)h^2D$ (with D the width of the plate). On the other hand the surface energy gained during this displacement, assuming the shape of the volume does not change, is $\sigma D dx$. Finally the ratio of the two energies gives the following Capillary number: $Ca = \tau_c h/\sigma$. We expect that capillary effects will be negligible if Ca is much larger than 1. Thus, for sufficiently high yield stress capillary effects become negligible. However, since from experimental data Ca is of the order of 1 (for millimetric coated layer and a yield stress of a few tenths of pascals) a further analysis of the results (see below) will be needed to conclude that capillary effects are in general negligible.

In order to appreciate the relative impact of gravity and viscous effects, it is particularly interesting to look at the flow characteristics of a YSF along an inclined plane of slope i with regards to a horizontal plane. We consider a uniform flow which, as a consequence, is a simple shear with a velocity $v(y)$ (where y is the distance from the plane) in the direction x of steepest slope. The shear rate is thus $v'(y)$. From momentum equation we deduce the shear stress distribution $\tau(y) = \rho g(h-y)\sin i$, where h is the thickness of the fluid layer. This implies that the maximum shear stress is reached along the wall ($y=0$) : $\tau_p = \rho g h \sin i$.

From these equations we deduce that the fluid remains in its solid regime in the region $y_c < y < h$, with $y_c = h - (\tau_c/\rho g \sin i)$ and flows in its liquid regime for $y < y_c$. The solid

region along the free surface is thus transported by the liquid layer along the plate. The thickness of this liquid layer decreases when the yield stress increases and finally the minimum layer thickness for a flow to take place is $h_c = \tau_c / \rho g \sin i$, which in the case of a vertical plate writes:

$$h_c = \frac{\tau_c}{\rho g} \qquad (2)$$

The validity of this description was checked for moderate slopes, typically smaller than 30° [27], but for this study we carried out additional specific tests by inclining a plate covered with a Carbopol gel layer up to $i = 90°$ which showed that, as expected from this straightforward theory, as long as the fluid adheres on the vertical plate the equation (2) rather well predicts the critical thickness.

For simple YSF, since the static and the dynamic yield stresses are identical this critical thickness is both the one beyond which the flow starts and the one at which it stops flowing if the fluid progressively drains (decreasing its thickness). Note that if $h < h_c$ the shear stress at the wall is everywhere lower than τ_c, so that the material remains in a solid state along the plate. As a consequence the layer can take any non-uniform shape $h(x)$ as long as $h(x) < h_c$. Finally we see that there is a natural length scale associated with the flow of a yield stress fluid over a vertical plate, namely h_c, which makes it possible to consider the dimensionless number $G = h/h_c$. When $G >> 1$ the fluid is mostly in its liquid regime, whereas when $G \approx 1$, it is mostly in its solid regime. Note that a complete integration of the momentum equation taking into account the constitutive equation (1) makes it possible to find the average flow velocity as a function of the fluid characteristics and layer thickness. This may be expressed as a relation between G and Bi [28].

2.4 First attempt of theoretical description

Since capillary effects are negligible for sufficiently high yield stress it is useful to review first the dip-coating of a Newtonian fluid (of viscosity η) when only viscous and gravity effects play a role, as it can serve as a reference for analyzing the case of YSF. An asymptotically uniform layer of thickness h_∞ is expected to form, which may be expressed as

$$h_\infty = \alpha \sqrt{\frac{\eta V}{\rho g}} \qquad (3)$$

with the value for α depending on the authors. This expression simply reflects some balance between a characteristic gravity stress ($\rho g h_\infty$) and a characteristic viscous stress ($\eta V / h_\infty$). In the aim of determining the value of α, Derjaguin and Levi [15] developed an elegant approach which provides interesting physical arguments in view of extending it to more complex fluid types. It consists first in considering that a uniform flow along the vertical plate leads to a flow rate $\rho g h^3 / 3\eta$ (as directly deduced from momentum equation), so that if such a flow occurs

along a plate moving steadily at a velocity V (tending to induce an upwards mass flux Vh) the net vertical flow rate per unit plate width will be

$$Q = Vh - \frac{\rho g h^3}{3\eta} \qquad (4)$$

Then it is assumed that the effective fluid thickness is such that this flow rate reaches its maximum ($(dQ/dh)_{h_\infty} = 0$), so that h_∞ is given by (3) with $\alpha = 2/3$. However numerical simulations [29] showed that the effective value for α is a priori smaller (i.e. 0.58).

Derjaguin and Levi [15] extended this approach to YSF now taking into account capillary effects. They focused on the case $Bi \to \infty$, so that the shear stress in the liquid regions is approximated by the yield stress. First of all they demonstrate that, in steady state, a uniform fluid layer in its solid state is formed along the plate at some distance above the bath. Then, from the momentum equation in the transition region, they deduce the stress distribution as a function of the pressure gradient (related to the free surface curvature) which, along the wall, gives the following equation:

$$\sigma \frac{d^3 h}{dx^3} + \rho g - \frac{\tau_c}{h} = 0 \qquad (5)$$

In the case of negligible capillary effects this equation reduces to $h = h_c$. This result may be seen as consistent with the above analysis as it maximizes the flow rate [15]. Such a result is in fact quite natural: it would be obtained by assuming that by withdrawing the plate from the bath we first tend to extract all the material of the bath because it is initially a solid, but eventually gravity limits the coated thickness by inducing a flow which ends up at a thickness equal to its maximum possible value in the solid state along the plate. Actually we will see below that the bath does not behave as an amount of fluid freely flowing relatively to the plate.

Finally, in the case of dominant capillary effects, i.e. $\tau_c << \sqrt{\rho g \sigma}$, Derjaguin and Levi [15] found

$$h_\infty \approx 13 R^3 \frac{{\tau_c}^2}{\sigma^2} \qquad (6)$$

3. Analysis from experimental data and numerical simulations

3.1 Experimental data

For the analysis in this paper we will rely on the existing data [16, 24] and on additional data obtained from similar experiments with different materials. The published data concern Carbopol gels, which from careful rheometrical tests (see [31]) appear to be simple YSF well represented by a HB model with a similar value of $k/\tau_c \approx 0.55$ and $n = 0.35$. Here we carried out additional tests with the same material type but at different concentrations, leading to different yield stress values, so that the final range of yield stresses covered in the present analysis will be [8-82 Pa]. Note that for one of these materials ($\tau_c = 34\,\mathrm{Pa}$) we found

$k/\tau_c \approx 0.41$. In the paper these different Carbopol gels will be referred to through their yield stress value. Moreover we carried out tests with three other YSF: an inverse emulsion and two mixtures of Glycerol and Carbopol, which will be referred to as CG. The continuous phase of the inverse emulsion is dodecane (7% wt.) with Span80 as surfactant. The aqueous phase (water + 45% wt. of dissolved calcium chloride) represents 85% of the total volume. Its rheological parameters are $\tau_c = 62\,\text{Pa}$, $k = 13\,\text{Pa.s}^n$ and $n = 0.45$. CG was prepared by mixing 90% in volume of glycerol with water. Then 0.3% (or 0.5%) in mass of Carbopol 980 powder is dissolved in the mixture. The dissolution of the Carbopol powder in glycerol is much longer than in water so the fluid is neutralized the following day with soda, becoming a gel. The rheological parameters of the CG are (for 0.3%) $\tau_c = 27\,\text{Pa}$, $k = 78\,\text{Pa.s}^n$ and $n = 0.42$ and (for 0.5%) $\tau_c = 40\,\text{Pa}$, $k = 88\,\text{Pa.s}^n$ and $n = 0.44$. The resulting high value for k/τ_c results from the large viscosity of the interstitial liquid of the gel. This will in particular allow to look at dip-coating flows at relatively small Bingham number.

Measurements were carried out under the conditions and with the procedures described in [24]. The coated thickness was measured from a succession of tests, weighting the mass (which very rapidly reached a plateau) of the plate coated with fluid after withdrawal for different depths of penetration. This mass was shown to be proportional to the penetration depth, proving the uniformity of the layer thickness, as confirmed by force measurement during withdrawal [24].

Note that the measurements are somewhat noisy, which may be expressed as an uncertainty of the order of 20% on the coated thickness. This is likely due to slight geometrical imperfections in the initial configuration and to the exact initial stress distribution inside the material in the solid state inside the bath, which cannot be perfectly controlled. However the time of rest before starting the test had no impact on the uniform thickness obtained in the stationary regime within the general uncertainty on data [24]. Finally we could just conclude that we do not perfectly control the state of the material in the bath but we did not identify clear trends which could explain the fluctuations from one measure to another.

Also note that for CG the weighted mass tends to a plateau after a longer time. In that case we just determined the thickness form the mass measured a short time after withdrawal, with the same timing as for other YSF (this point will be discussed further below). For transparent materials (Carbopol gels and CG) the flow field inside the bath was determined by PIV, using 80 μm-diameter polystyrene beads dispersed in the fluid as tracers (see [30]). Particle motions were observed in a vertical plane perpendicular to the solid plate and along its central axis, illuminated with a 20 mW continuous red laser sheet. A CCD camera attached to the container recorded the particle displacements along the plate during all the duration of its withdrawal

until the plate disappeared off the picture. The velocity field is determined over a single side of the plate. An experiment represents the study of the plate displacement over a distance of about 15cm. The analysis lied on a cross-correlation technique with the commercial software DaVis. To limit the noise and to make easier the comparison of the data, the velocity fields were computed by averaging the pictures taken during a 1cm displacement of the plate.

3.2 Numerical simulations of the flow in the bath

The experimental data were completed with numerical simulations that rely on the second order cone programming (SOCP) for which dedicated interior point solvers are available. This technique is part of the "non-regularizing methods" that aim at solving the original non-smooth viscoplastic problem. More precisely, the simulations are based on a finite element discretization of the 2D fluid domain using a quadratic interpolation of the velocity field inside each triangular element. The energy minimum principle is then discretized and the minimization problem is reformulated in a form suitable for the SOCP solver Mosek [31]. More details on the numerical implementation and the validation of the technique for the simulation of yield stress fluid flows can be found in [32-33].

In the present case the fluid semi-domain is schematized by a rectangle minus the (rectangular) volume occupied by the semi-plate on one side. Thus we here do not describe the free surface flow along the plate outside the bath, and even neglect its possible impact on the rest of the flow (we will see later in this paper that this assumption is valid). Since the system is symmetrical only half of the fluid domain is modelled. The symmetry implies that the normal velocity and the shear stress along the side plane (the plane along the mid-plate) of this half-domain are equal to zero. A perfect adherence of the fluid along the container walls and along the plate surface is assumed. The plate velocity is V. The stress components along the free surface of the sample are equal to zero. A comparison with a series of velocity profiles obtained by PIV during such a flow showed a very good agreement between simulations and experimental data [32-33]. This allows us to be confident on the ability of this numerical approach to provide some systematic information concerning the flow characteristics inside the bath. In particular this led us to test the impact of the container size and to explore a wider range of Bingham numbers. Note that all equations explicitly mentioned in the text can be solved analytically while for numerical simulations the momentum equations were solved numerically.

3.3 Basic qualitative trends of dip-coating with yield stress fluids

The global characteristics of dip-coating with yield stress fluids do not differ from dip-coating with simple liquids: the bath essentially remains macroscopically at rest (i.e. the material remains inside the container) while a layer of fluid is withdrawn with the plate. This means that the material undergoes, at least in some regions, a solid-liquid transition, otherwise it would all

remain stuck to the plate and the container. The main difference between YSF and simple liquids lies in the fact that, after an initial transient stage the coated layer is uniform (see Figure 1) and fixed to the moving plate, i.e. the fluid coated to the plate is in its solid regime. Note that a full experimental demonstration of the uniformity of the coated thickness was provided in [24]. The thickness of this uniform layer will be noted h_∞. In our range of experimental conditions this thickness increases monotonously with the plate velocity, we did not observe a decrease larger than the uncertainty on data.

However this uniform thickness is obviously not reached immediately. The transient regime, i.e. the flow characteristics before reaching a uniform layer along the withdrawn plate, was studied in depth in [24]. In this work it was shown that the weight of material coated on the plate after complete withdrawal increases linearly with the initial length of immersion when this length is larger than 3-4 cm. This means that a uniform layer thickness is reached along the plate at a distance larger than 3-4 cm from the top line of contact. This result was in agreement with direct qualitative observation of the layer thickness. Moreover it was shown that after some distance of withdrawal the force needed to extract the plate varies linearly, and along approximately the same period the velocity profile along the plate inside the bath evolves and reaches a steady shape after a displacement of about 4 cm from the initial position. These different information converge to the conclusion that there is a transient regime both inside and outside the bath which, with our boundary conditions, ends after a distance of displacement of the order of 3-4 cm, and a uniform layer thickness is then reached. In the present work we will focus on the stationary flow associated with a uniform coated thickness and study it as a function of rheological and boundary conditions.

3.4 Flow regimes

Let us first look at the variations of the coated layer thickness as a function of the Capillary number. In Figure 2 we choose to represent data for velocities in a range of low values in order to limit the impact of the shear-dependent component of the constitutive equation. This means that we look at results for which the yield stress component is dominant, i.e. Bingham numbers much larger than 1. Under these conditions the main rheological parameter is the yield stress and as a first approximation the velocity has a negligible impact. Note that for each yield stress value the data are aligned but due the relatively larger uncertainty on data, the points corresponding to increasing velocities in this range are not aligned in the order of increasing velocity but instead are dispersed along this fictive line.

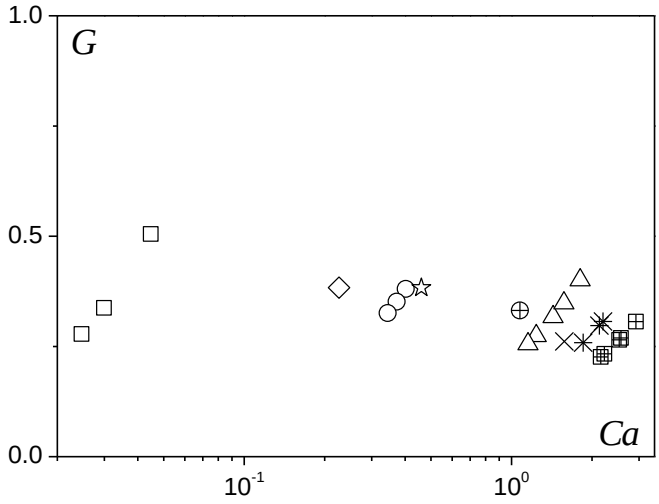

Figure 2: Gravity number as a function of Capillary number for dip-coating experiments in the lowest velocity range, i.e. [0.2-2 mm.s-1], for YSF (Carbopol gels) with different yield stresses: 8 Pa (squares), 20 Pa (diamond), 27 Pa (circles), 29 Pa (stars), 48 Pa (cross-circle), 56 Pa (triangles), 65 Pa (cross), 71 Pa (asterisks), 82 Pa (cross-squares).

The first result (see Figure 2) is that at low velocities the coated thickness scaled by the critical thickness for a free surface gravity flow is almost constant for Ca between 0.1 and 3. This suggests that in this range capillary effects are negligible and the coated thickness essentially results from the balance of viscous and gravity forces. As a consequence capillary effects should a fortiori be negligible at higher velocities since in that case the viscous stress is larger while capillary effects remain more or less constant. From the data of Figure 2 it seems possible that capillary effects start to play a significant role for Ca <0.1. Finally for Ca between 0.1 and 3 the thickness is a result of some equilibrium between gravity and viscous effects, and since we have $G \approx 0.3 \pm 33\%$ in this range (the last data point on the left in Figure 2 is out of this range) we deduce that as a rough approximation the coated thickness at low velocities may be expressed as:

$$h_\infty \approx 0.3 \frac{\tau_c}{\rho g} \qquad (7)$$

It is remarkable that this value is more than three times lower than the critical thickness for a free surface flow stopping along a vertical plate, i.e. h_c, given by (4). This has two important implications:

1) The final thickness does not at all correspond to the maximum possible thickness associated with a simple free surface flow under gravity (in contrast with Derjaguin and Levi conclusion [15]).
2) The bath tends to strongly limit the coated thickness.

Let us now examine the impact of velocity. More generally we look at the role of the shear-dependent component in the constitutive equation, which is quantified by the Bingham number. In that aim all our data are plotted in a diagram G vs Bi^{-1} (in which we used the coated thickness as characteristic length in the Bingham number). In consistency with the above result we again find an apparent plateau around $G = 0.3$ at sufficiently large Bi (say larger than 1), despite significant data scattering around this value. In fact we will see later that this large scattering partly finds its origin in the fact that the above description is not fully consistent, i.e. the coated thickness cannot be simply described through a single relationship between G and Bi^{-1}. This inconsistency of this representation for example appears from the very different coated thicknesses obtained at low Bi^{-1} with the emulsion and a Carbopol gel despite similar yield stress values.

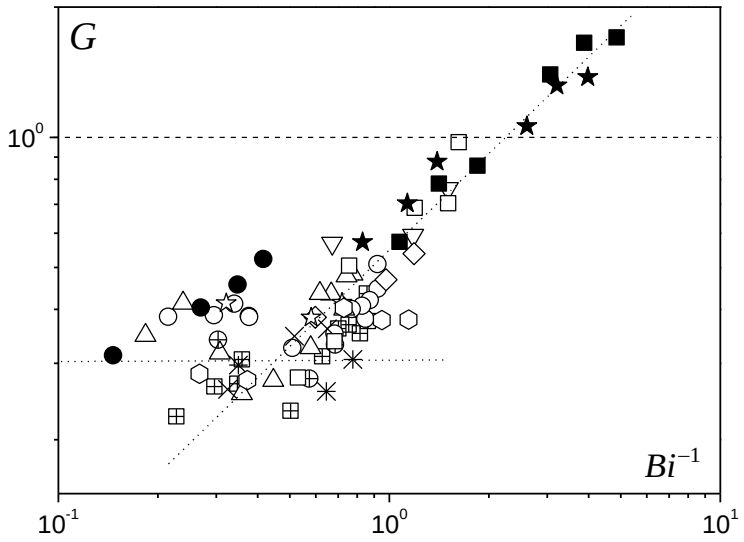

Figure 3: Gravity number as a function of the inverse of the Bingham number for all the dip-coating experiments in yield stress fluids. Same symbols as in Figure 2 plus additional symbols for: Carbopol, 69 Pa (hexagons), 9 Pa (inverse triangles), CG 27 Pa (filled squares) and 40 Pa (filled stars), and emulsion, 63 Pa (filled circles). The horizontal dotted line corresponds to equation (7), the inclined dotted line to a power-law with an exponent 0.75.

Nevertheless we can see some general trends from Figure 3. First of all the variations of the coated thickness with the plate velocity are rather slow. That means that over about 4 decades of velocities the thickness varies by a factor of the order of 10. Here we recognize the effect observed with any type of flow with YSF (see [1]): any variable, such as a lengthscale, pressure drop or stress, varies very slowly with the flow rate, generally in a way similar to the variations of the shear stress vs shear rate in the constitutive equation.

Another conclusion from Figure 3 is that when the Bingham number becomes sufficiently low, say typically below 1, we have another regime in which the dimensionless thickness significantly increases with Bi^{-1}. It is worth noting that here we can observe data (with CG) with $G>1$. This means that in the corresponding experiments the fluid was in fact not completely rigid along the plate, it was still somewhat draining as for simple liquids. However, due to the large values for k/τ_c in that case the asymptotic thickness (i.e. h_c) is not yet reached and our measurement procedure which here provides the thickness just after withdrawal is close to that used for simpler liquids. It is interesting to note that this regime may be well represented (see Figure 3) by a straight inclined line corresponding to $G = Bi^{-m}$ (with $m = 0.75 \pm 0.5$). This leads to a dependence of the form $h_\infty \propto V^{0.25}$ (for $n = 0.45$). Remarkably this result is close to, and thus consistent with, the semi-empirical prediction of Gutfinger and Tallmadge [8] for weakly elastic shear-thinning power law fluids for negligible capillary effects: $h_\infty \propto V^{n/1+n}$, which gives $h_\infty \propto V^{0.31}$ for $n = 0.45$.

Finally these results only constitute a first approach of the problem of dip-coating with yield stress fluids. Indeed we were able to distinguish some critical unexpected trends, i.e. existence of two regimes, coated thickness significantly smaller that obtained for a free vertical stoppage, but several aspects remain problematic and suggest that the representation of data in Figure 3 does not reflect all the aspects of the problem: in the regime of large Bingham number the dispersion of data around a possible master curve cannot be explained only by the uncertainty on measurements; the coated thickness smaller than h_c means that the bath plays a significant role; a master curve in the form G vs Bi, using the coated thickness, would mean that the physical process is independent of what occurs in the bath. It follows that we now need to have information about the flow inside the bath and how it can impact the coating process.

3.2 What does happen in the bath?

General characteristics

Several important characteristics of the flow field around a plate moving (penetration or extraction) through a bath of yield stress fluid were observed through experiments with different Carbopol gels [16, 24, 29]:

- Rapidly after the beginning of plate motion the fluid flows in its liquid regime inside a uniform and constant layer thickness along the plate (except close to the edges) while it is solid outside (see Figure 4); this conclusion was reached by following the total deformation undergone by fluid elements along their trajectory: the solid region corresponds to a total deformation saturating in time, while liquid region corresponds to a total deformation continuously increasing [29]; for any other test the apparent thickness of the liquid region was estimated from the intersection between the apparently sheared zone and the horizontal plateau;

- In this liquid layer the flow is uniform: it was shown that the velocity profile along most of the immersed part of the plate is constant [29];
- This thickness increases slowly with the plate velocity and is independent of the yield stress of the fluid as long as the ratio k/τ_c remains constant [24, 29].
- These flow characteristics are almost similar (although opposite) for a plate penetrating or a plate extracted from the fluid; in penetration the liquid thickness appeared to be smaller of about 30% than during extraction [24].

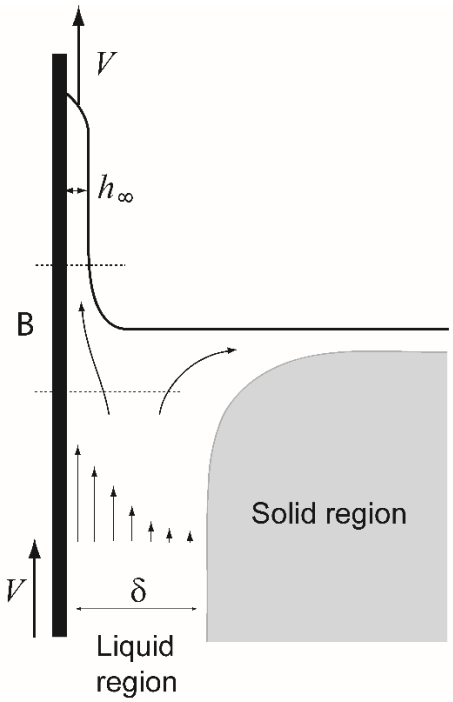

Figure 4: Scheme of the flow field during dip-coating of YSF. The grey area corresponds to the solid region, in which the elements undergo only limited deformations. The rest of the fluid is in its liquid regime, undergoing large deformations mostly at a constant shear rate (in the uniform region).

In order to explore a wider range of parameters (i.e. velocity, rheological parameters, boundary conditions) we carried out a more systematic study via numerical simulations. The overall aspect of the low field was similar to that observed by PIV (see [16, 24]), leading to a similar distinction between liquid and solid regions. As a consequence here the variations of the flow characteristics are mainly discussed through the evolution, along the plate, of the profile of the vertical velocity component. The important new information provided by these simulations are as follows:

1) A uniform flow along the plate in the bath starts to develop when the immersed length of the plate is larger than the width of the fluid container, i.e. when the fluid can be

considered to be effectively "confined" between the two solid planes; the characteristics of this uniform flow are independent of the distance of the plate tip from the container bottom as long as this distance is much larger than the plate thickness;

2) This uniform flow takes place along the plate at a distance of the order of the liquid layer thickness from the plate tip and from the free surface; it is independent of the plate thickness as long the distance from the container sides is much larger than this thickness (i.e. $e < L/10$);
3) Flow characteristics are similar whether or not gravity is taken into account; they are also similar during penetration ($V < 0$) and extraction ($V > 0$); this means that gravity does not play any role in the flow problem inside the bath; as a corollary, this suggests that elastic effects in the solid regime, which are not taken into account in these simulations, and act differently in penetration and extraction, might be at the origin of the slight difference observed experimentally in the uniform flow profiles in these two flow types (see above);
4) Since gravity does not play any role, the momentum equations can be rescaled by the yield stress, which implies that in the simulations the flow characteristics only depend on the ratio k/τ_c, the velocity and the boundary conditions;
5) When the aspect ratio of the container (L/H) is varied, the flow characteristics remain qualitatively similar but the liquid layer thickness increases with this aspect ratio; we nevertheless did not explore this aspect in more detail as it is a huge problem (impact of the aspect ratio when varying other parameters, impact of the container shape, etc); here we will thus only describe the characteristics of the liquid layer for boundary conditions corresponding to our experimental ones, and then study the dip-coating characteristics when varying the rheological parameters and the velocity under given bath conditions.

Note that point 3) contradicts the simple model suggested in [16] for predicting the thickness of the liquid layer in the bath and which was based on the assumption of a balance between gravity and viscous effects.

Under these conditions, for a given aspect ratio L/H, the flow characteristics will only depend on the Bingham number, with here $Bi_L = (\tau_c/k)(V/L)^n$. Looking at the velocity profiles in the uniform region in a wide range of Bingham numbers we see that they rapidly vary for Bi_L larger than 0.1 but approximately exhibit a constant shape with a finite (non-zero) sheared thickness for smaller Bi_L (see Figure 5). Actually these velocity profiles are similar when rescaled by a characteristic length δ (see inset of Figure 5). Similar velocity profiles are also obtained for aspect ratio L/H in the range [0.3-1.8].

Detailed characteristics of the uniform flow

Since we are dealing with uniform flows in some significant fluid volume, it is possible to describe analytically the flow characteristics in these regions [30, 34-35]. Let us recall the main lines of this approach. In such a uniform flow along the plate the only non-zero velocity component (u) is along x and only depends on the distance from the plate y. This is a simple shear, for which the only non-zero tangential component of the stress is $\tau_{xy} = \tau(y)$, and the momentum equation is thus:

$$0 = -\frac{\partial p}{\partial x} + \frac{\partial \tau}{\partial y};\ 0 = -\frac{\partial p}{\partial y} \tag{8}$$

with, in the frame of reference attached to the plate assuming no wall slip, the boundary conditions: $u(y=0) = 0$ and $u(y \to \infty) = V_0$, where V_0 is the velocity of the solid region. We deduce from (8) that the pressure is constant in each plane x =Cst and that the pressure gradient along x is constant. After integration we get $\tau(y) = \tau_w - (\tau_w - \tau_c)y/\delta$ for $0 < y < \delta$ where $\tau_w = \tau(y=0)$ is the shear stress at the wall and:

$$\delta = -\frac{\tau_w - \tau_c}{\partial p/\partial x} \tag{9}$$

Equating the shear stress with that given by the HB constitutive equation of the material in the liquid regime (1) we find an expression for the shear rate $\dot{\gamma} = du/dy$ which may be integrated to give the velocity profile: $u = V_0 - V_0(1 - y/\delta)^{1+1/n}$; or, equivalently, in the frame of reference of the solid region:

$$v = V_0(1 - y/\delta)^{1+1/n} \text{ for } 0 < y < \delta \tag{10}$$

We then deduce $\tau_w = \tau_c + k\dot{\gamma}_w^{\,n} = \tau_c\left[1 + \alpha Bi_\delta^{\,-1}\right]$, in which we used $\alpha = m^n$ and introduced the Bingham number: $Bi_\delta = \tau_c / k(V/\delta)^{-n}$. Using the above results we find the expression for the pressure gradient as a function of the layer thickness, the velocity and the rheological parameters:

$$\frac{\partial p}{\partial x} = -\alpha \frac{\tau_c}{\delta} Bi_\delta^{\,-1} \tag{11}$$

Although we are able to describe the shape of the velocity profile the fundamental problem of such a flow is that $\partial p/\partial x$ is a given external constant which is unknown so that δ is unknown too, and as yet we are not fully quantitatively predictive.

The velocity profile (10) predicted by this approach is in excellent agreement with the velocity profiles obtained from simulations (see inset of Figure 5). Note that for this comparison we had to compute V_0 from V, after measuring the plateau velocity v_0 (which is negative in our frame of reference): $V_0 = V - v_0$. Also note that δ is larger than the apparent thickness of the liquid layer as it was measured so far (see above), because the velocity profile includes a large region in which the velocity and the shear rate are much lower than along the plate, a region which may be as a first approximation considered as the beginning of the solid region.

Now it is interesting to compare all our velocity profiles, obtained for extraction tests either during this study or the previous one [24], with this general equation (10), by fitting δ. There is some scattering but the agreement with the theoretical prediction is again excellent (see Figure 6). Curiously the agreement is also very good between all the data obtained with the CG and the theoretical velocity profile for $n = 0.35$ (instead of the profile associated with $n = 0.42$ as they should) (see Figure 6). We do not have a clear explanation for that.

Finally we can plot the value for δ as a function of Bi_L (see Figure 7) obtained from simulations and from experiments. We see that there is a good agreement between these two sets of data, the remaining discrepancy likely having its origin in the various uncertainties in measurements and fitting procedure. In the following we will consider that the data obtained from simulations as the reference value for δ. In the range [8-30 mm] these data can be well represented by the following model:

$$\delta = \delta_c + 40 Bi_L^{-1} \qquad (12)$$

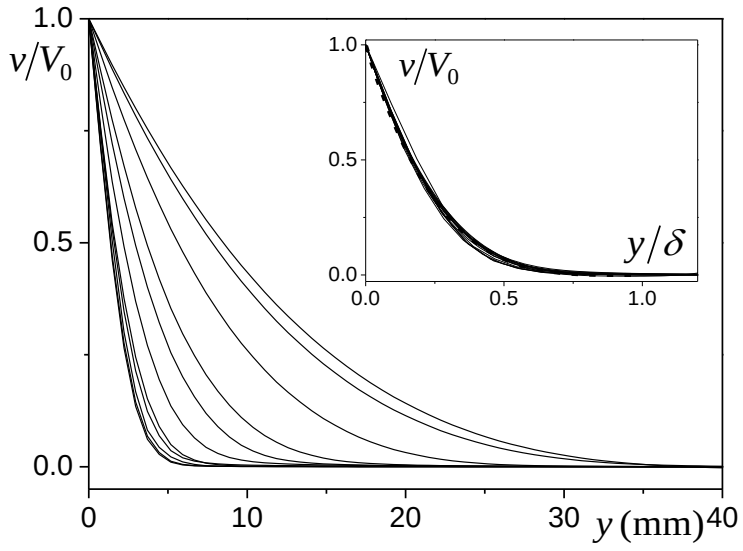

Figure 5: Uniform velocity profile (numerical simulation) in the sheared layer along the plate inside the bath for different Bi_L values: (from left to right) 8.8×10^{-4}, 1.7×10^{-3}, 8.8×10^{-2}, 4.4×10^{-2}, 0.12, 0.22, 0.32, 0.7, 1.1, 5.5, 27.6. The inset shows the same profile when the distance from the plate is rescaled by a parameter δ (see values in Figure 7).

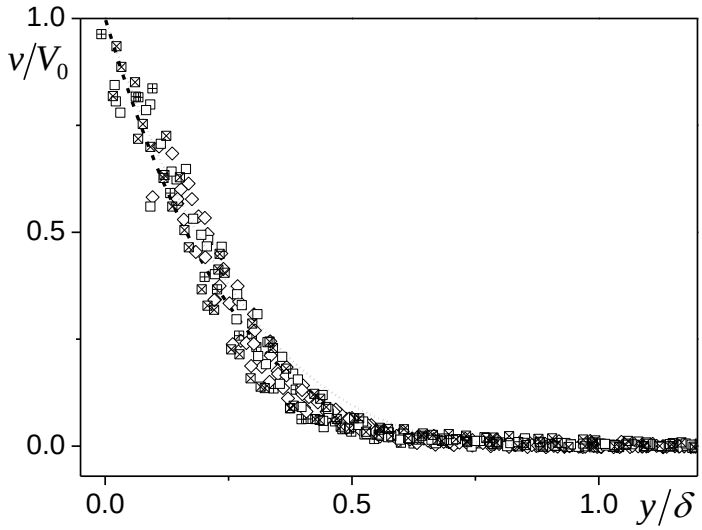

Figure 6: Velocity profile in the uniform flow region along the plate in the bath, as measured by PIV, as a function of the distance rescaled by a parameter δ (see values in Figure 7) for different fluids and plate velocities (V): Carbopol gels: ($\tau_c = 8\,\mathrm{Pa}$) from 0.2 to 17 mm.s^{-1} (open squares), ($\tau_c = 34\,\mathrm{Pa}$) from 0.8 to 17 mm.s^{-1} (crossed squares), ($\tau_c = 71\mathrm{Pa}$) from 0.2 to 17 mm.s^{-1} (diagonal crossed squares); CG from 0.2 to 17 mm.s^{-1} (diamonds). The velocity represented here is the relative velocity between the fluid and the solid region rescaled by the relative velocity between the plate and the solid region. The dashed line is equation (10) with $n = 0.35$ and the dotted line is the same equation with $n = 0.42$.

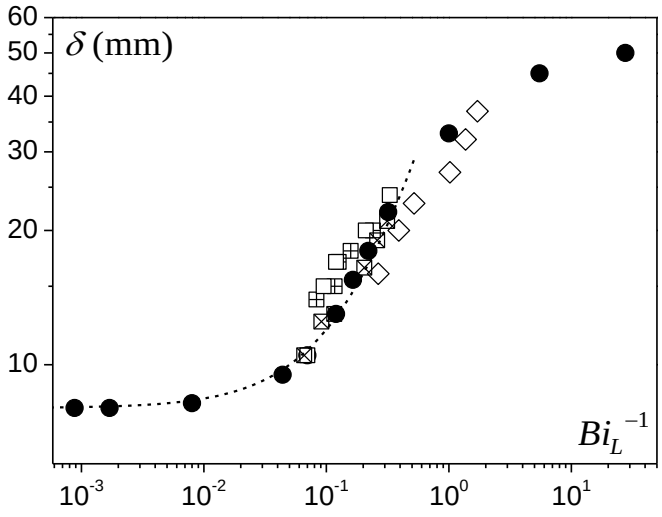

Figure 7: Thickness of the liquid layer in the bath as a function of the inverse of the Bingham number determined from rescaling of numerical profiles (filled circles) of Figure

5 and experimental profiles of Figure 6 (with the same symbols as in this figure). The dotted line corresponds to equation (12).

4. Dip-coating and flow in the bath

We now have a complete view of the main flow characteristics in the bath and along the plate. The plate motion through the bath induces a shear flow localized in a layer of thickness δ. Since the characteristics of this flow are almost independent of the plate direction they are independent of the possible flow and deposit occurring outside the bath along the plate. Actually the flow in the bath has a critical impact on the coating. The displacement of the plate inside the bath sets up the fluid in some specific distribution of states: we have a volume of fluid remaining in its solid regime and which will not supply any material to the coating. The coated layer is formed from the fluid of the bath in the liquid regime, more precisely from the vertical liquid layer along the plate.

This in particular makes it possible to determine an upper bound for h_∞: if we assume that all the fluid in the liquid layer is then coated to the plate we find from the mass conservation:

$$h_{\infty,\max} = (1/V_0)\int_0^\delta v(y)\,\mathrm{d}\,y = \frac{\delta}{2+1/n} \qquad (13)$$

For n around 0.4 or lower this value is significantly lower than the value which would be obtained for a homogeneous simple shear, i.e. $\delta/2$. This is due to the large, very slowly sheared region for $y/\delta > 0.5$, which corresponds to a fluid volume which will likely remain in the bath. Finally, considering the above result and the shape of the velocity profiles we can approximate the velocity profile in the liquid layer as a simple shear in a thickness $\lambda = 2h_{\infty,\max}$.

In the above approach the mass flux ($h_{\infty,\max}V$) of the liquid layer inside the bath along the solid region entirely coats the plate, thus inducing a flux $h_\infty V$. In fact there is a region (B in Figure 4) of transition between the uniform flowing region along the plate, imposed by the presence of the solid region in the bath, and the solid layer stuck onto the plate. In this region of transition the fluid is no more confined between the plate and the solid region, but progressively turns from its liquid to its solid regime. This flow is rather complex but as a first approximation we will consider it as a vertical free surface flow under gravity. This yields a flow of fluid which reduces the mass of material finally fixed on the plate, somewhat as in the approach of Derjaguin and Levi for simple liquids (see above). The fraction of mass flux eventually remaining in the bath will then feed the horizontal flow at the free surface of the bath (see the right side in Figure 4).

It is rather difficult to determine the characteristics of the flow in the transition region since the apparent viscosity of the fluid in this layer is heterogeneous and evolves along region B. In

order to get a rough estimation of this mass flux we will make the following assumptions: we have in the region B a uniform layer of a Newtonian fluid of thickness λ flowing freely under gravity along the plate; the viscosity of this fluid results from the simple shear in the liquid layer inside the bath in a region of thickness, i.e. $\eta = \tau/\dot{\gamma}$ with $\dot{\gamma} = V/\lambda$. The flow rate in this region is thus given by $\rho g \lambda^3 / 3(\tau/\dot{\gamma})$. Considering the approximation made with regards to reality we can expect that the effective flux should be given by this expression times a factor α to be determined. Finally the difference between the vertical flux ($h_\infty V$) at a large height and the vertical flux along the liquid layer along the solid region inside the bath is equal to this counter flux, so that after elimination of V we get:

$$h_\infty = \frac{\lambda}{2} - \frac{\alpha \rho g \lambda^2}{3\tau} \tag{14}$$

From this expression we deduce that this approach is not valid for too small yield stress values, which may lead to negative values for h_∞. In fact, for low yield stress (say < about 25 Pa) it is likely necessary to take into account capillary effects.

The parameter λ in equation (14) is deduced from an expression of the type (12) for δ. We thus see that the final coated thickness is mainly governed by the flow inside the bath. From the constitutive equation (1) the shear stress in the second term writes $\tau = \tau_c \left(1 + Bi_\lambda^{-1}\right)$ in which here $Bi_\lambda^{-1} = (k/\tau_c)(V/\lambda)^n$. The impact of the yield stress lies in the second term: for example when the yield stress tends to infinity the second component of the right-hand-side tends to zero, so that we have $h_\infty \approx h_{\infty,\max}$; if on the contrary the yield stress is low the second term is large, a significant amount of liquid is left in the bath, and the coated thickness is significantly smaller than $h_{\infty,\max}$. Finally equation (14) predicts that the thickness of the coated layer will tend to a finite value when the velocity tends to zero (i.e. Bi_λ^{-1} and Bi_L^{-1} tend to zero): $h_{\infty,c} = \lambda_c/2 - \alpha \rho g \lambda_c^{\,2}/3\tau_c$, in which we noted $\lambda_c = 2\delta_c/(2 + 1/n)$. We in particular deduce that this approach is not valid when according to this expression the coated thickness is negative, i.e. when $\tau_c/\rho g < 2\alpha\lambda_c/3$.

In Figure 8 we can see that for $\tau_c > 25\,\text{Pa}$ we have a good agreement between the theoretical prediction (14) and our data, by taking $\alpha = 0.6$. For smaller yield stress the predicted coated thickness is negative (e.g. for $\tau_c = 8\,\text{Pa}$) or significantly lower than the experimental one (see data for $\tau_c = 21\,\text{Pa}$ in Figure 8). For all larger yield stress values there is a scattering of data in a zone of $\pm 30\%$ the exact agreement, but there is no specific trend leading to some discrepancy: the data appear to be effectively dispersed at random around the expected value, and this level of uncertainty seems consistent with the different uncertainties in measurements which play a role in this comparison (uncertainty on liquid layer thickness estimation, on coated thickness measurement, and on the rheological parameters). On the contrary in Figure 3 the scattering around some master curve was so large that the discrepancy could reach 70%. Moreover it is worth emphasizing that the theoretical expression (14) is able to predict the coated thickness

layer of both the Carbopol gels and the emulsion (see Figure 8), which are materials exhibiting significant differences in their rheological behaviour. At last we also plotted the data for the CG. In that case λ was computed directly from the data for δ since with this material we are in the region where the expression (12) does not predict experimental data (see Figure 7). Moreover, as mentioned above, we can suspect that the coated layer was still slowly flowing along the vertical plate during measurements, which means that the above approach should be at least slightly modified to take into account this effect. Despite this complication it is remarkable that we get an excellent agreement between the theoretical prediction and the data for CG by using only a different value for α, now taking $\alpha = 0.4$. This means that this model is robust, as long as the yield stress of the material is sufficiently large it is able to predict the reality for more complex conditions on the basis of the same physical ingredients.

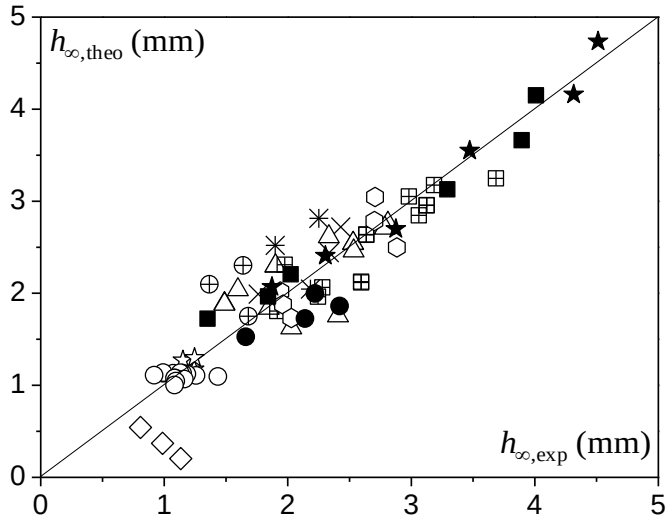

Figure 8: Coated layer thickness predicted by the model (see text, equation 14) as a function of the measured thickness. Same symbols as in Figure 3. The continuous line corresponds to a perfect agreement between theory and experiments.

Conclusion

From previous data completed by additional experiments and numerical simulations we were able to identify the main processes taking place during the dip-coating of a yield stress fluid. In particular we showed that the flow inside the bath, and essentially the liquid region formed due to the plate motion, plays a critical role on the value of the thickness of the uniform layer finally coated to the plate. On the basis of these detailed information, we could finally suggest a simple model describing the coated thickness as a function of the rheological parameters and the boundary conditions. The weakness of this model lies in the description of the flow in the

transition region between the liquid layer at some depth inside the bath and the rigid layer along the plate, which could not be predicted exactly (a single arbitrary coefficient had to be introduced). Further information on the flow characteristics in this region would be needed to improve the model. However it is remarkable that we were able to predict very well (despite the inherent uncertainty on data) the data for yield stress larger than 25 Pa, for different materials (Carbopol gels at different yield stresses, emulsion, CG) and in a range of velocities of two decades. This means that despite a strong simplification of the description of the flow characteristics we capture the main physical mechanisms of the process: the coated layer results from the upper flow within the liquid layer inside the bath minus a counter flux resulting from the action of gravity in the transition region.

A critical aspect that we did not tackle seriously here is the exact impact of the container size. It was indeed shown that the container size has an impact on the liquid layer thickness inside the bath, which was demonstrated to be at the origin of the coated thickness. It is thus likely that the aspect ratio of the container (L/H) plays a significant role on the coated thickness. Further experiments and simulations are needed in that field.

Since for yield stress fluids the flow in the bath plays a major role in the formation of the coated layer the state of the fluid in the bath might play an important role and it could be interesting to precisely control or even have an action on the material in the bath while withdrawing the plate. In particular we can expect that if we fully liquefy the fluid in the bath, for example by simultaneously mixing it strongly, the coated layer would be different and finally closer to that expected for a simple shear-thinning fluid (i.e. without yield stress). This is an interesting perspective, but this certainly requires significant or tricky experimental developments. This idea was suggested by an anonymous referee.

Acknowledgements: We are grateful to Xavier Chateau for fruitful discussions.

References

[1] P. Coussot, Yield stress fluid flows: A review of experimental data, *J. Non-Newt. Fluid Mech.*, 211, 31-49 (2014)

[2] K.J. Ruschak, Coating flows, *Ann. Rev. Fluid Mech.*, 17, 65-89 (1985)

[3] D. Quéré, Fluid coating on a fiber, *Ann. Rev. Fluid Mech.*, 31, 347-384 (1999)

[4] J. H. Snoeijer, J. Ziegler, B. Andreotti, M. Fermigier, and J. Eggers, Thick films of viscous fluid coating a plate withdrawn from a liquid reservoir, *Phys. Rev. Lett.*, 100, 244502 (2008)

[5] H. C. Mayer, R. Krechetnikov, Landau-Levich flow visualization: Revealing the flow topology responsible for the film thickening phenomena, *Phys. Fluids*, 24, 052103 (2012)

[6] F. Kamisli, Free coating of a non-Newtonian liquid onto walls of a vertical and inclined tube, *Chem. Eng. Processing*, 42, 569-581 (2003)

[7] R.W. Hewson, N. Kapur, P.H. Gaskell, A model for film-forming with Newtonian and shear-thinning fluids, *J. Non-Newt. Fluid Mech., 162*, 21 (2009)

[8] C. Gutfinger, J.A. Tallmadge, Films on non-Newtonian fluids adhering to flat plates, *AIChE J.*, 11, 403 (1965)

[9] K. Afanasiev, A. Münch, B. Wagner, Landau-Levich problem for non-Newtonian liquids, *Phys. Rev. E*, *76*, 036307 (2007)

[10] R.P. Spiers, C.V. Subbaraman, W. Wilkinson, Free coating of non-Newtonian liquids onto a vertical surface, *Chemical Engineering Science*, *30*, 379-395 (1975)

[11] A. de Ryck, D. Quéré, Fluid coating from a polymer solution, *Langmuir*, 14, 1911-1914 (1998)

[12] J. Ashmore, A.Q. Shen, H.P. Kavehpour, H.A. Stone, G.H. McKinley, Coating flows of non-Newtonian fluids: weakly and strongly elastic limits, *J. Eng. Math.*, 60, 17-41 (2008)

[13] P. Hurez, P.A. Tanguy, *Polymer Eng. Sci.*, Finite-element analysis of dip coating with Bingham fluids, 30, 1125-1132 (1990)

[14] A. Filali, L. Khezzar, E. Mitsoulis, Some experiences with the numerical simulation of Newtonian and Bingham fluids in dip coating, *Computers & Fluids*, 82, 110-121 (2013)

[15] B.V. Derjaguin, S.M. Levi, *Film coating theory* (The Focal Press, London, 1964)

[16] M. Maillard, J. Boujlel, P. Coussot, Solid-Solid Transition in Landau-Levich Flow with Soft-Jammed Systems, *Phys. Rev. Lett*., 112, 068304 (2014)

[17] P. Coussot, H. Tabuteau, X. Chateau, L. Tocquer, and G. Ovarlez, Aging and solid or liquid behavior in pastes, *J. Rheol.*, 50, 975-994 (2006)

[18] P. Coussot, Q.D. Nguyen, H.T. Huynh, and D. Bonn, Viscosity bifurcation in thixotropic, yielding fluids, *J. Rheol*., 46, 573-589 (2002)

[19] P. Coussot, G. Ovarlez, Physical origin of shear-banding in jammed systems, *European Physical Journal E*, 33, 183-188 (2010)

[20] G. Ovarlez, S. Cohen-Addad, K. Krishan, J. Goyon, P. Coussot, On the existence of a simple yield stress fluid behavior, *J. Non-Newt. Fluid Mech*., 193, 68-79 (2013)

[21] N.J. Balmforth, I.A. Frigaard, G. Ovarlez, Yielding to Stress: Recent Developments in Viscoplastic Fluid Mechanics, *Ann. Rev. Fluid Mech*., 46, 121-146 (2014)

[22] P. Coussot, *Rheometry of pastes, suspensions and granular materials* (Wiley, New York, 2005)

[23] J. Boujlel, P. Coussot, Measuring yield stress: a new, practical, and precise technique derived from detailed penetrometry analysis, *Rheol. Acta*, 51, 867-882 (2012)

[24] M. Maillard, J. Boujlel, P. Coussot, Flow characteristics around a plate withdrawn from a bath of yield stress fluid, *J. Non-Newt. Fluid Mech.*, 220, 33-43 (2015)

[25] J. Boujlel, P. Coussot, Measuring the surface tension of yield stress fluids, *Soft Matter*, 9, 5898-5908 (2013)

[26] L. Jorgensen, M. Le Merrer, H. Delanoe-Ayari, C. Barentin, Yield stress and elasticity influence on surface tension measurements, *Soft Matter*, 11, 5111-5121 (2015)

[27] P. Coussot, S. Boyer, Determination of yield stress fluid behaviour from inclined plane test, *Rheologica Acta*, 34, 534-543 (1995)

[28] P. Coussot, Steady, laminar, flow of concentrated mud suspensions in open channel, *J. Hydraulic Res.*, 32, 535-559 (1994)

[29] B. Jin, A. Acrivos, A. Münch, The drag-out problem in film coating, *Phys. Fluids*, 17, 103603 (2005)

[30] J. Boujlel, M. Maillard, A. Lindner, G. Ovarlez, X. Chateau, P. Coussot, Boundary layer in pastes-Displacement of a long object through a yield stress fluid, *J. Rheol., 56*, 1083-1108 (2012)

[31] Mosek, The Mosek optimization toolbox for Matlab manual (MOSEK ApS, Denmark, 2008)

[32] J. Bleyer, M. Maillard, P. De Buhan, P. Coussot, P., Efficient numerical computations of yield stress fluid flows using second-order cone programming, *Computer Methods in Applied Mechanics and Engineering*, *283*, 599-614 (2015)

[33] M. Maillard, Spreading of yield stress fluids, Ph.D. thesis, Univ. Paris-Est, 2015 (in French)

[34] J.D. Oldroyd, 2-Dimensional plastic flow of a Bingham solid – A plastic boundary-layer theory for slow motion, *Proc. Cambridge Philosophical Soc.*, 43, 383-395 (1947)

[35] J.M. Piau, K. Debiane, The adhesive or slippery flat plate viscoplastic boundary layer for a shear-thinning power-law viscosity, *J. Non-Newt. Fluid Mech.*, 117, 97-107 (2004)